Rev. Cub. Fis. vol. 27, No. 2B, 2010. p.275-279
ISSN: 0253-9268. Original paper
Paper from Tecnolaser 2009

Revista Cubana de Física
Calle I No. 302 e/ 15 y 17
Vedado, La Habana. CP 10400
www.fisica.uh.cu/biblioteca/revcubfi/index.htm

Implementation of an optical coherence tomography system for painting characterization*

Hannah U. K. S. Kashyap[a, b], Cláudia C. B. O. Mota[b], Bernardo B. C. Kyotoku[b], Plínio B. Santos-Filho[c], and Anderson S. L. Gomes[b]

a) Photonova Inc, 110 Elm Crescent, Baie D'Urfé (QC) H9X 2P6, Canada.
b) Department of Physics. Universidade Federal de Pernambuco, Cidade Universitária 50670-901, Recife, PE, Brazil; anderson@df.ufpe.br†
c) Agency for Studies and Heritage Repair, Jardim Atlântico 52050-250, Olinda, Brazil.
† Corresponding author

Received: 2/06/10. Approved in final version: 25/11/10.

Abstract. Optical Coherence Tomography (OCT) is a new but well established imaging technique for medical diagnosis, which can produce two- or three-dimensional images of bio-tissues with a few μm spatial resolution. Its potential as a non-invasive tool for art conservation of paintings and other objects has been realized recently. In this work, we report the implementation of two OCT systems applied to painting characterization. One system operates in the so-called spectral domain, with a central wavelength of 840 nm and axial resolution of 10μm. The second system has its central wavelength at 1280 nm, with spatial resolution of 20μm, and operates in the time domain. Both systems are independently controlled and have imaging software developed in-house using LabView. Using both systems, a 15 years old acrylic portrait has been analyzed, where the paint layers, light and dark colors, and the cotton threads of the canvas could be identified.

Sumario. La tomografía de coherencia óptica (OCT) es una técnica nueva, pero bien establecida para hacer imágenes para el diagnóstico médico. Puede producir imágenes de los bio-tejidos en dos o tres dimensiones con una resolución espacial de pocos milímetros. Su potencial como una herramienta no invasiva para la conservación de pinturas de arte y otros objetos se ha realizado recientemente. En este trabajo, se presenta la ejecución de dos sistemas de OCT aplicados a la caracterización de pinturas. Un sistema opera en el denominado dominio espectral, con una longitud de onda central de 840 nm y 10 μm de resolución axial. El segundo sistema tiene su longitud de onda central en 1280 nm, una resolución axial de 20 μm, y opera en el dominio del tiempo. Ambos sistemas son controlados independientemente y usan un software en LabView desarrollado en nuestro laboratorio.

Keywords. Optical tomography, 42.30.Wb, laser applications 42.62.Cf.

* ***Editor's note:*** *Even though this paper was originally sent to Tecnolaser 2009, it was not possible to include it in the special number devoted to the conference (vol. 27, 1, 2010). Its refereeing has been full responsibility of the Tecnolaser Organizing Committee.*

1 Introduction

Artwork examination is carried out routinely in galleries and museums for conservation purposes as well as for cultural heritage diagnostics.[1] However, in the past, destructive methods such as stratigraphy were used to gather information about paint layer thickness and inner painting structure to build a tomographic form of paintings.[2, 3] This approach requires tiny sections of paintings to be removed, usually from cracks or the painting's periphery. These are then polished to recreate a cross-sectional sample of the varnish layer and studied under a microscope to analyze paint layers, identify pigments used, or pinpoint signs of deterioration or previous restoration.[1, 4] This method is not desirable as it is invasive and information collected in this way is not representative of the whole painting. Consequently, there has been much interest in non-invasive optical imaging techniques for artwork diagnostics of paint layers or for tomographic imaging. Raman Spectroscopy,[5] UV fluorescence,[6] IR reflectography,[7] are a few examples. However each method has its drawbacks. For instance, the former method is difficult to apply to larger objects such as paintings[8] and the information provided by the latter two techniques is either restricted to imaging the surface, or integrates over the thickness of the sample.[9]

The novel non-invasive Optical Coherence Tomography (OCT) technique is a high resolution approach which can be used for painting characterization. As with IR reflectography, preparative under-drawings beneath the painted layers can be visualized.[10] Furthermore, OCT can be used for preventive conservation of artwork through identification of thinning varnish layers, early signs of deterioration and cracks with micrometer resolution. OCT is a real-time technique, which uses visible or near-infrared light to provide cross-sections of semi-transparent or scattering media.[11] The bandwidth of the source determines the axial resolution which can be of the order of 1-2µm. As such, OCT is also particularly suited to bio-medical applications and has been widely used in clinical practice in ophthalmology.[12]

Since the absorption and scatter in pigments is sensitive to wavelength and longer wavelengths are able to penetrate more deeply, the use of wavelengths in the region of 1.5-2.5µm may be beneficial.[9] However, in order to maintain high resolution, the bandwidth needs to be very large. Here, we use OCT systems centered on two different wavelengths, 840nm and 1280nm, for painting characterization through investigation of tomographic painting structure and paint layer thickness and analysis of preparatory under-drawings.

2 Experimental setup

Two domains were used in this experimental setup: the spectral domain and the time domain. Time domain OCT (TD-OCT) was introduced[13] in 1991. In TD-OCT, the optical delay line arm basically consists of either a movable arm or a Fourier domain delay line.[14] A major advantage of the time domain OCT instrument is its simple basic design and essentially unlimited depth of imaging, which depends only on the range of movement of the reference mirror.[9]

The theoretical basis for spectral domain OCT (SD-OCT)[15] was published only two years after that of time domain OCT. In contrast to TD-OCT, information about the entire axial structure of the object analyzed is collected simultaneously in one "shot" of the CCD camera. This information is encoded in the frequency signal. It is stored and subsequently decoded by numerical (reverse) Fourier transformation, conveniently performed on a personal computer.[9] It has been shown more recently that SD-OCT has several advantages over the TD-OCT,[16] including sensitivity[17] and fast data acquisition, and since the first report on imaging implementation[18] its use has been widespread.[14, 17, 19]

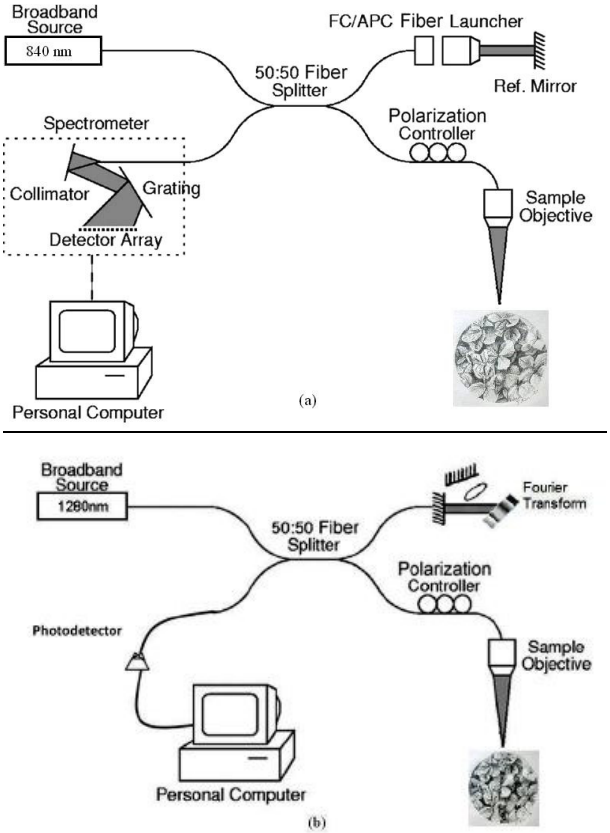

Figure 1: Schematic setup of (a) SD-OCT 840 nm and (b) TD-OCT 1280 nm.

The basic theory of SD-OCT is well known[15]. For clarity, we introduce some of the basic physics of the technique. Considering E(t) as being the input light's electric field, the electric field in the output port of the interferometer can be modeled as being:

$$E_{out}(t) = \sqrt{K_r}E(t-\tau_r) + \sum_i \sqrt{K_i}E(t-\tau_i) \qquad (1)$$

In Eq. (1) Kr, (Ki) is the fraction of input light power that was reflected at a point r, (i) back to the interferometer, τr, (τi) is the time of flight the light takes to go from an input point to the point r, (i) and then to the output. The subscript r refers to the reference arm and i refers to a point in the sample. The output is the autocorelation of the electric field function:

$$\Gamma_{out}(t)=\left[K_r+\sum_i K_i\right]\Gamma\left(t+\sum_{i\neq j}\sqrt{K_iK_j}\Gamma(t-\Delta\tau_{j,i}\right)+ \\ +\sum_i\sqrt{K_iK_\gamma}\Gamma(t-\Delta\tau_{\gamma,i})+\sum_i\sqrt{K_iK_\gamma}\Gamma(t+\Delta\tau_{j,i}) \quad (2)$$

In Eq. (2), Γ(t) is the autocorrelation function of the input light and Δτn,m = τm - τn. Since the input light has a large bandwidth then, due to the uncertainty principle which leads to the time-bandwidth product being a constant, Γ(t) is a near delta function at the origin. In Eq. (2), the first two terms are parasitic terms that must be removed. The last terms contain the information about the sample and are symmetric quantities. Since τr is constant, it can be seen that in each of the two last terms there is going to be a peak centralized at Δτr,i, with an amplitude proportional to the square root of the fraction of light power that returned from the sample from point i. Using the Wiener– Khinchin theorem by taking the Fourier transform of the power spectrum density Gout(υ) of the light coming out of the interferometer, one can arrive at the autocorrelation function. This function has a central peak, which corresponds to a parasitic term of Γ_{out}, where as the other two symmetric peaks are the last two terms in Eq (2). The parasitic peak and one of the symmetric peaks are removed by taking a second spectrum $G^{\pi/2}_{out}$ of the output light, but with the mirror displaced by λ/8, causing the phase shift of π/2 in the fringes. The relation:

$$\Gamma=\left\|FT\left[G_{out}+iG^{\pi/2}_{out}\right]-FT\left[G^{\pi/2}_{out}+iG_{out}\right]\right\|+ \\ +\left\|FT\left[G_{out}+iG^{\pi/2}_{out}\right]\right\|-\left\|FT\left[G^{\pi/2}_{out}+iG_{out}\right]\right\| \quad (3)$$

where FT denotes the Fourier transform and || || is the complex number normalization. This therefore, allows a high discrimination signal to be obtained without parasitics. The resolution in depth can be calculated from the expression shown in equation 4 below:

$$\Delta Z = 0.44\lambda^2/\Delta\lambda \quad (4)$$

here λ is the central wavelength and Δλ is the bandwidth of the spectrum.

We used two OCT experimental setups: 1280 nm, in time domain (TD-OCT), and 840 nm, in spectral domain (SD-OCT). The SD-OCT setup uses a broadband light source (superluminescent diode, Broadband SLD Lightsource S840, SUPERLUM, Moscow, Russia) operating at 840 nm and with a spectral width of 50 nm and a fiber output power 25mW (Figure 1a). The system is based on the Michelson interferometer set-up: in the reference arm, there is a mirror mounted on a piezoelectric base; in the sample arm, a mirror controlled by a Galvo motor is required for the scanning of light at the sample. A beam splitting mirror first splits light from the source. It then travels down the reference and sample arms, respectively. The reflected and back-scattered light coming from both arms is then recombined at the beam splitter and collected by a spectrometer, consisting of a lens collimator system, 1200 l/mm grating, and an optical detector (linear CCD cam, ATMEL, 2048 pixels, 12 bits, California, United States), connected to a computer. The system is controlled by the software OCT 800 – Complex Square, developed from LabView program language, that collects data and generates the image. The image acquistion time is less than one second.

The TD-OCT setup uses a broadband light source (superluminescent diode, SLD-571, SUPERLUM, Moscow, Russia) operating at central wavelength of 1280 nm, with a bandwidth of 64.6 nm and a fiber output power 5mW (figure 1b). As with the SD-OCT 840 nm, the system is based on a Michelson interferometer, but in this setup, the delay line is in the Fourier domain[14] consisting of a grating and a scanning galvo. In the sample arm, there is a motor which moves to perform the lateral scanning. The recombined beams are fed into a photodetector and associated electronics, and the output is sent to a computer with a software OCT 1300 MC3, a LabView based imaging program.[20]

Figure 2. Portrait of Lucian Freud, painted with acrylic by Plinio Santos-Filho, 1995.

3 Results and discussion

The portrait of Lucian Freud is a 15 year old acrylic painting by Plínio Santos-Filho. The piece measures 25 x 20 cm, and the areas scanned by OCT are indicated on

the image (see figure 2). The painting is acrylic on canvas which is mounted on cardboard.

Some parts of the acrylic painting were selected to demonstrate the capabilities of OCT for nondestructive analysis of paintings. Images were obtained by collecting adjacent nondestructive tomographic slices (A-Scans) by scanning 10 mm in the transverse direction. In the axial direction, depths ranging from some tens to hundreds of µm were investigated by scanning with the reference arm.

As mentioned earlier, the resolution of the SD-OCT system is dependent on the bandwidth of the source and can be calculated using Eqn 4. Our SD-OCT system had a measured experimental resolution of 10 µm, although using equation 4 we calculate a theoretical limit of 6.2 µm. For the TD-OCT the measured experimental resolution was 20 µm, although the calculation reveals a theoretical limit of 11.2 µm. This deviation from the theoretical limits for spatial resolution could be due to many reasons including unknown refractive index of the different paint mixtures, dispersion in the paints and differential spectral absorption which would degrade the OCT signals.

Figures 3 and 4 correspond to the selected region in original painting (see figure 2), which were then scanned by each OCT system.

From our measurements, the maximum probed depth at 1280nm is ~2mm in the material (not correcting for the refractive index). At 840nm the maximum probed depth is of the same order, keeping in mind that the real depth will be different when corrected for with the refractive index.

Images obtained with OCT 1280 nm in the time domain (see figure 3), show the surface characteristics and the difference between light and dark colors. The regions that are painted white (see figures 3a and 3b) contain zinc oxide acrylic paint. We are also able to distinguish different layers of paint using both OCT systems. Using TD-OCT, this is most easily seen in figure 3b. Here, the last white layer painted on the nose is seen as an elevated band on the tomographic image. The thickness of this extra layer of paint can be determined as 286 µm.

Images obtained with OCT 840 nm in the spectral domain, are presented in figure 4. These images, created by laterally combining the adjacent A-scans, also show distinct regions and layers of acrylic paint. This is most easily seen in the area indicated in figure 4b. At greater axial depths, additional inner-painting structure can be visualised. In fact, the cotton fibers of the canvas are seen at the center of the images as a dotted vertical line. We are not able to detect this when using 1280nm OCT in the TD. There is always a balance between the light penetration depth and the maximum resolution obtained. Although TD-OCT 1280nm penetrates the sample more deeply, the resolution of SD-OCT 840nm is greater. Hence, only using SD-OCT 840nm are we able to see the cotton fibers below the paint layers. Care must be exercised to avoid mistaking the image artifacts, as pointed out in figure 4b.

Despite some of the shortcomings of the systems discussed in this article, OCT systems operating at two different wavelengths can provide excellent, detailed information of the underlying textures of paintings and canvases. It is interesting to note that the ability to detect and localise an internal structure of paintings may even allow the detection of forgeries or the authentication of originals. For example. an original painting could be deliberately embedded with a microscopic tag at a hidden location. An OCT system could later be used to certify the painting's authenticity.

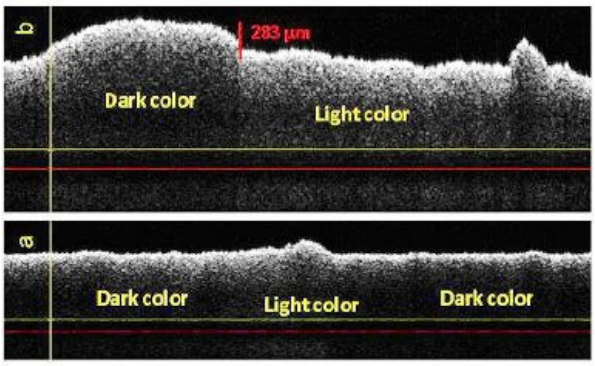

Figure 3: TD-OCT 1280 nm images results

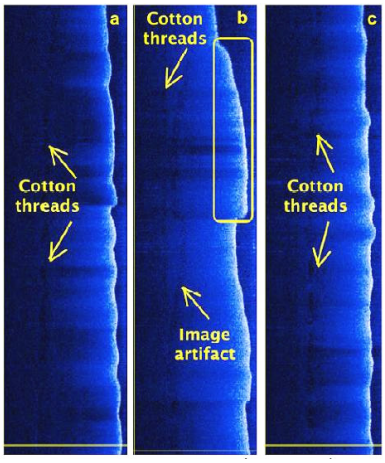

Figure 4: SD-OCT 840 nm images results

4 Conclusion

In this study, we carried out a comparison between the TD-OCT and the SD-OCT applied to painting characterization. The features pointed out, which were known by the artist of the painting, were identified in both setups, except for the cotton fibers, which could be seen only with the 840nm SD-OCT. This can be due to the better resolution of the system or the wavelength used. Therefore, we conclude that both OCT systems must be used in combination to gain a better understanding and more accurate picture of the texture, internal structure and characteristics of paintings. The results in this article are typical of several samples we have investigated.

By employing the OCT technique, it is possible to determine the material's refractive index,[21] which will be

very useful information for painting characterization and artwork diagnostics. This work is under way in our laboratory.

As multipurpose OCT devices are already commercially available, it has also been demonstrated that fieldwork can be exploited, without the need to remove the painting or the artifact being analyzed to a laboratory.

Acknowledgments

The authors from Universidade Federal de Pernambuco wish to thank CNPq, CAPES, and FACEPE, Brazilian Agencies, for financial support and scholarships. They are also part of the Center of Excellence in Nanophotonics and Biophotonics (PRONEX Program, FACEPE/CNPq) and the Photonics National Institute of Science and Technology (CNPq/MCT), to whom the support is also acknowledged.

References

1. H. Liang, S. Martin-Simpson, A. Podoleanu and D. Saunders, "Optical coherence tomography: a non-invasive technique applied to painting conservation," SPIE Newsroom, DOI: 10.1117/2.1200601.0067.

2. T. Arrechi, M. Bellini, C. Corsi, R. Fontana, M. Materazzi, L. Pezzati, and A. Tortora. "A New Tool for Painting Diagnostics: Optical Coherence Tomography," Optics and Spec., 101(1), 23-26 (2006).

3. L. Bonizzoni, S. Caglio, A. Galli, G. Poldi, "A non invasive method to detect stratigraphy, thicknesses and pigment concentration of pictorial multilayers based on EDXRF and vis-RS: in situ applications," Appl. Phys. A. 92(1), 203-210 (2008).

4. P. Targowski, B. Rouba, M. Gora, L. Tyminska-Widmer, J. Marczak, A. Kowalczyk, "Optical coherence tomography in art diagnostics and restoration," Appl. Phys. A. 92(1), 1-9 (2008).

5. M. Castillejo, M. Martín, D. Silva, et al., "Laser-induced breakdown spectroscopy and Raman microscopy for analysis of pigments in polychromes," Journal of Cultural Heritage. 1(1). S297–S302 (2000).

6. D. Comelli, C. D'Andrea, G. Valentini, R. Cubeddu, C. Colombo, and L. Toniolo. "Fluorescence Lifetime Imaging and Spectroscopy as Tools for Nondestructive Analysis of Works of Art" Appl. Opt. 43(10). 2175-2183 (2004).

7. Walmsley, C. Metzger, J. K. Delaney, and C. Fletcher, "Improved visualization of underdrawings with solid-state detectors operating in the infrared," Studies in Conservation. 39(4), 217–231 (1994).

8. P. Vandenabeele, F. Verpoort, L. Moens, "Non-destructive analysis of paintings using Fourier transform Raman spectroscopy with fibre optics," Journal of Raman Spectroscopy. 32(4), 263-269 (2001).

9. P. Targowski, M. Góra, and M. Wojtkowski, "Optical Coherence Tomography for Artwork Diagnostics," Laser Chem., 2006. Article ID 35373, 11 pages (2006).

10. M. Attas et al. "Near-infrared spectroscopic imaging in art conservation: Investigation of drawing constituents," Journal of Cultural Heritage. 4(2), 127-136 (2003).

11. B. J. Rouba et al. "Optical coherence tomography fornon-destrcutive investigations of structure of objects of art," 9th International Conference on NDT of Art, Jerusalem Israel, 25-30 May 2008. Accessed March 2009.

12. L. L. Otis, M. J. Everett, E. S. Sathyam, and B. W. Colston, Jr, "Optical coherence tomography: A new imaging technology for Dentistry" JADA. 131, 511-514 (2000).

13. D. Huang, E. A. Swanson, C. P. Lin, J. S. Schuman, W. G. Stinson, W. Chang, M. R. Hee, T. Flotte, K. Gregory, C. A. Puliafito and J. G. Fujimoto, "Optical coherence tomography," Science. 254(5035), 1178–1181 (1991).

14. N. Cense, T. Nassif, M. Chen, S. H. Pierce, B. Yun, B. Park, G. Bouma and J. Tearney, "Ultrahigh-resolution high-speed retinal imaging using spectral-domain optical coherence tomography," Optics Express. 12(11), 2435-2447 (2004).

15. T. Dresel, G. Hausler and H. Venzke, "Three-dimensional sensing of rough surfaces by coherence radar," Applied Optics. 31(7), 919–925 (1992).

16. B.B.C. Kyotoku and A.S.L. Gomes, "Dental fiber-reinforced composite analysis using optical coherence tomography," Opt. Commun. 279(2), 403-407 (2007).

17. R. Leitgeb, C. Hitzenberger and A. Fercher, "Performance of fourier domain vs. time domain optical coherence tomography," Optics Express. 11(8), 889-894 (2003).

18. M. Wojtkowski, A. Kowalczyk, R. Leitgeb and A. F. Fercher, "Full range complex spectral optical coherence tomography technique in eye imaging," Optics Letters. 27(16), 1415-1417 (2002).

19. Y. Yasuno, S. Makita, T. Endo, M. Itoh, T. Yatagai, M. Takahashi, C. Katada and M. Mutoh, "Polarization-sensitive complex Fourier domain optical coherence tomography for Jones matrix imaging of biological samples," Applied Physics Letters. 85, 3023 (2004).

20. D. D. D. Fonsêca, B. B. C. Kyotoku, A. M. A. Maia and Anderson S. L. Gomes, "In vitro imaging of remaining dentin and pulp chamber by Optical Coherence Tomography: comparison between 850nm and 1280nm," accepted to Journal of Biomedical Optics, 2009.

21. P. H. Tomlins, W. M. Palin, A. C. Shortall and R. K. Wang, "Time-resolved simultaneous measurement of group index and physical thickness during photopolymerization of resin-based dental composite," Journal of Biomedical Optics. 12(1), 1-7 (2007).